© Pol J Radiol 2023; 88: e343-e348
DOI: https://doi.org/10.5114/pjr.2023.130252

Received: 02.06.2023
Accepted: 20.06.2023
Published: 28.07.2023

Polish Journal of Radiology

http://www.polradiol.com

Original paper

Assessment of sodium (^{23}Na) brain MRI at 3T – preliminary results

Pawel Wawrzyniak[1,B,D,E], Anna Hebda[1,A,C], Aleksandra Awramienko-Włoczek[1,C,F], Patrycja Mazgaj[1,B,C], Sylwia Heinze[2,E,F], Barbara Bobek-Billewicz[1,A]

[1]Maria Sklodowska-Curie Memorial Cancer Centre and Institute of Oncology, Gliwice Branch, Poland
[2]Maria Sklodowska-Curie Memorial Cancer Centre and Institute of Oncology, Cracow Branch, Poland

Abstract

Purpose: The purpose of this work was to establish a database of tissue sodium concentration (TSC) in the normal brain of healthy volunteers. Tissue sodium concentration can be used as a sensitive marker of tissue viability in stroke or radiation therapy monitoring.

Material and methods: Thirty-seven volunteers were scanned with a ^{23}Na protocol in the span of one year; within this group, 29 studies were of acceptable quality. The study was approved by the Local Bioethics Committee. Data were acquired during a single magnetic resonance (MR) scanner session. The single scanner session consisted of ^{23}Na 3D radial gradient echo (GRE) acquisition, MPRage, SPACE-FLAIR, and Resolve-DTI. MPRage images were segmented to obtain masks of the grey matter (GM), white matter (WM), and cerebrospinal fluid (CSF), which were registered to the sodium image space for image analysis. Images were transformed into TSC maps – a signal calibration curve obtained from the reference phantom of known sodium concentration and known relaxation time.

Results: The collected data were analysed in 2 different ways: volunteers were divided by sex and by age. No significant differences in TSC were found between sexes. In all comparisons there was a significant difference in TSC between younger and older volunteers. In healthy volunteers mean TSC were as follows: GM 33.21 ± 4.76 mmol/l, WM 28.41 ± 4.03 mmol/l and for CSF 41.3 ± 6.69 mmol/l.

Conclusions: This preliminary work is a base for further work with sodium imaging in brain lesions. The entirety of the collected data will be useful in the future as a baseline brain TSC for comparison to values obtained from pathologies.

Key words: MR-imaging, sodium MRI, brain/brain stem, adults.

Introduction

Magnetic resonance imaging (MRI) employs the nuclear magnetic resonance (NMR) principle to obtain diagnostic information about biological tissues. Every nuclei with non-zero spin can be used for MRI; however, because of its natural abundance and high sensitivity to external magnetic fields, hydrogen is the most widely used. All the factors listed above amount to a high signal-to-noise ratio in hydrogen MRI (^{1}H-MRI). Superior tissue contrast is the reason why ^{1}H-MRI is used so extensively for soft-tissue imaging. Its ability to present anatomy is superb; however, some diseases have no anatomic findings visible or their presence is very late. Because most of the hydrogen signal comes from either fat or water, there is limited biochemical information that can be obtained with standard ^{1}H-MRI. There are techniques that extend ^{1}H-MRI capabilities in that regard, but these are also limited. There are some other nuclei with non-zero spin that can provide a window into crucial biochemical processes. They require additional hardware and often software. For example, phosphorus magnetic resonance spectroscopy (^{31}P-MRS) can provide information about tissue energy metabolism, phospholipids metabolism, and pH levels [1-3].

Correspondence address:
Sylwia Heinze, PhD, Maria Sklodowska-Curie Memorial Cancer Centre and Institute of Oncology, Cracow Branch, Poland,
e-mail: sylwia.heinze@onkologia.krakow.pl

Authors' contribution:
A Study design · **B** Data collection · **C** Statistical analysis · **D** Data interpretation · **E** Manuscript preparation · **F** Literature search · **G** Funds collection

Carbon MRI (^{13}C-MRI) can be used in metabolic imaging [4]. Helium (^{3}He) and xenon (^{129}Xe) can provide useful information about the lungs, which are normally outside the scope of MRI [5]. A drawback of all non-proton-based MRI techniques is a lower signal-to-noise ratio (SNR). In the case of sodium imaging, there is approximately 20,000 times less signal than in the case of ^{1}H-MRI. This is due to lower *in vivo* concentration than in the case of protons, and a lower gyromagnetic ratio.

Performing sodium (^{23}Na) MRI, tissue sodium concentration (TSC) maps can be obtained. These maps carry a plethora of useful clinical information on various tissues. A major role of sodium ions in the human body is managing membrane transport using an ionic pump and as a counter ion for balancing charges of tissue anionic macromolecules. As such, it provides information in various diseases that impact function of sodium-potassium ion pump or disrupt ion homeostasis.

It has been shown that ^{23}Na-MRI has its place in stroke management [6], as a marker of viable tissue (only after the acute stroke phase) prior to strokectomy performed in some cases due to brain swelling. When it comes to brain tumours, ^{1}H-MRI offers a number of useful modalities that provide indirect information about tumour characteristics. However, during radiation and chemotherapy the most important issue is the response to treatment. Here the non-quantitative nature of the ^{1}H-MRI signal is a drawback. Several imaging techniques, like dynamic contrast enhancement (DCE), dynamic susceptibility contrast (DSC), diffusion weighted imaging (DWI), and magnetic resonance spectroscopy (MRS), expand the capabilities of proton MRI, but their limitations can impair the radiologist's ability to correctly asses treatment response. Sodium MRI is quantitative in principle, and it has been shown that brain tumours have higher TSC than normal brain [7]. The same work points to another parameter derived from TSC and bound by some assumptions, namely cell volume fraction (CVF). Tissue sodium concentration and CVF together can evaluate extent of tumour better than conventional proton MRI [8]. It was also suggested that the prognostic potential of sodium MRI in brain tumours can be as good as isocitrate dehydrogenase (IDH) [9].

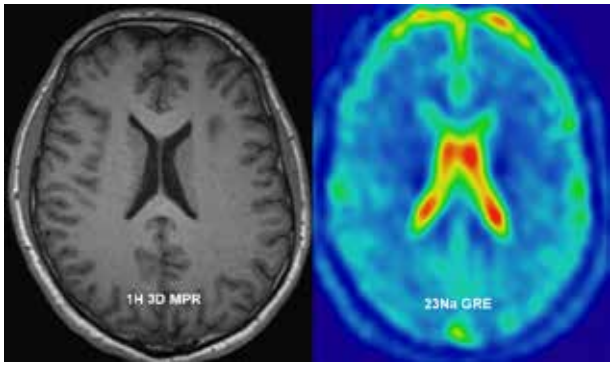

Figure 1. Example 3T MR brain images (^{1}H and ^{23}Na)

Sodium MRI has possible applications in various regions and pathologies. There are some reports of its usefulness in Alzheimer disease [10,11], kidney imaging [12], muscle pathology imaging [13], as well as body and spine imaging [14,15]. In this work, gradient echo (GRE) sequence was applied to acquire a signal used to reconstruct the TSC brain maps of healthy volunteers.

Material and methods

Magnetic resonance imaging (^{23}Na-MRI and ^{1}H-MRI) was performed on 37 volunteers between October 2017 and October 2018. The examined group consisted of 22 females and 15 males. The mean age of the combined group of men and women was 37 years (range 22-64 years). Twenty-nine out of the 37 studies were of acceptable quality and were processed. The remaining 8 of the 37 studies (22%) were rejected due to incomplete acquisition or artefacts caused by the patient's movement during the study.

All volunteers had an examination performed on a MAGNETOM Prisma 3T scanner (Siemens Healthcare, Erlangen Germany) with a double tuned ^{23}Na/^{1}H coil (RAPID Biomedical, Rimpar Germany), which allowed both proton and sodium imaging without moving the patient.

Sodium imaging (^{23}Na)

Gradient echo acquisition with radial readout scheme was performed with 4.7 mm isotropic resolution; field of view (FOV) – 300 × 300 mm, matrix (MTX) – 64; receiver bandwidth – 260 Hz/pixel; repetition time (TR) and echo time (TE) were, respectively, 100 and 2.87 ms with flip angle (FA) 90 degrees. A total of 16 slices were acquired. To achieve an acceptable signal-to-noise ratio (SNR) the acquisition was averaged (NA) 23 times, which resulted in 20 minutes of total acquisition time (Figure 1).

Proton imaging (^{1}H)

Additionally, to assess the anatomy and for segmentation purposes, high-resolution T1 MPRage sequence was performed with 0.9 mm isotropic voxel.

Post-processing

Two phantoms with known sodium concentration were positioned inside the coil for calibration. These phantoms were taped to the birdcage coil column close to the patient's temporal bone to capture them within the FoV. Those phantoms (2 standardized 100-ml conical tubes) contained 20 and 70 mM of sodium. Using the signal intensity of these phantoms (which corresponded to known sodium concentration) a linear curve was fitted to obtain scale factors between signal intensity and so-

dium concentration [16]. Using these factors all acquired sodium data were recalculated into TSC using ImageJ [17] software. Then all additional steps were taken to calculate TSC values specific for tissue. The unit of all obtained values is mmol/l.

The post-processing pipeline used to acquire TSC values started with denoising of raw sodium images by means of an optimized blockwise nonlocal means denoising filter [18] to remove excess noise present in the obtained data. A similar procedure was performed on anatomic imaging. For the next step, segmentation of white matter, grey matter, and cerebrospinal fluid was performed on MPRage sequence with Statistical Parametric Mapping (SPM [19]) software. SPM uses a segmentation process that performs tissue classification, bias correction, and image registration [20] using tissue probability maps and ICBM space template for European brains [21]. Then all the acquired images were normalised into the same space (they were stretched and translated until the anatomical structures on all images overlapped). That process enabled the use of white matter, grey matter, and CSF as masks on sodium images. Subsequently, values from all voxels inside a specific mask were gathered and processed to acquire the mean sodium concentration. This process was performed using Multi-Image Analysis GUI (Mango [22]). Mean values for white matter (WM), grey matter (GM), and cerebrospinal fluid (CSF) were obtained from all sodium images (Figure 2).

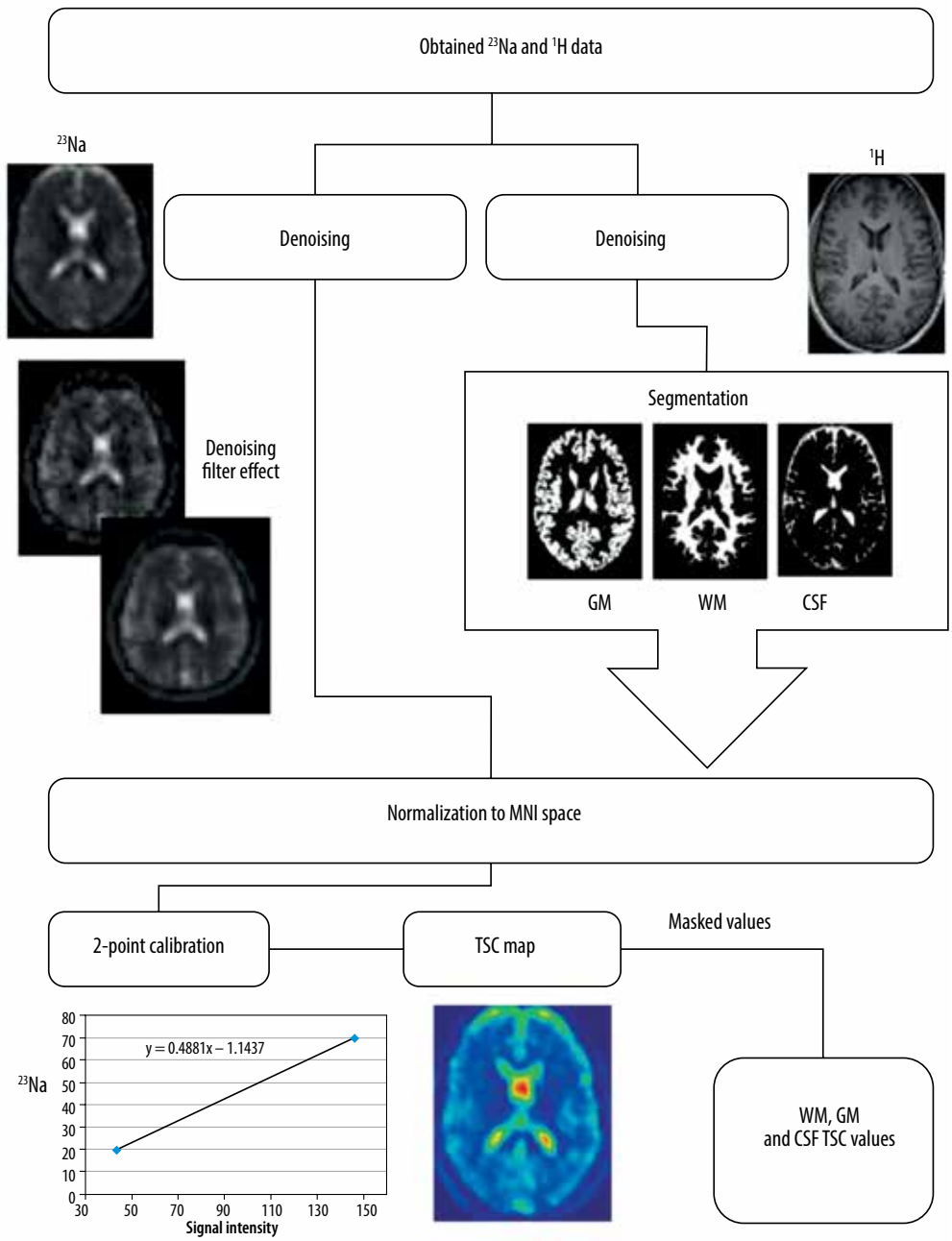

Figure 2. Data postprocessing pipeline

Statistical analysis

Data analysis was performed with Statistica 13 software. The statistical significance threshold was set at 0.05. To assess normal distribution the Shapiro-Wilk test was performed. A *t*-test was performed to compare differences between TSC of WM, GM, and CSF for the whole group. For subgroups, nonparametric tests were performed because the collected data did not follow the normal distribution. To determine if there were any differences within groups, Friedman ANOVA was performed with post-hoc test. The Kruskal-Wallis test was performed to evaluate the difference in parameter values in the groups divided by sex and age. All the box-and-whiskers plots were presented with mean values as a measure of central tendency. Standard error (SE) and 1.96*SE were presented as box and whiskers respectively. The collected data were analysed in 2 different ways to lead to conclusions. Firstly, all volunteers were divided by sex and secondly by age (more and less than 35 years). The age criterion was set to ensure roughly equal groups.

Results

Using the described method and data analysis allowed us to obtain brain TSC maps for WM, GM, and CSF. The distribution of all TSC values acquired for the whole group was deemed normal; however, when data were fragmented in both ways normal distribution criteria were not met (Figure 3). With no division into groups, statistically significant differences between all the tissues ($p < 0.001$) were observed (Figure 4). TSC in CSF was significantly higher compared to GM and WM ($p < 0.001$). TSC in WM had significantly the lowest concentration compared to the other groups ($p < 0.001$) (Table 1).

Volunteers were divided into groups by gender. Significant differences were found between all tissues (GM, WM, and CSF) in both groups ($p < 0.001$) (Figure 5). Comparing WM, GM, and CSF TSC between men and women yielded TSC WM in man vs. woman $p = 0.1439$, TSC GM $p = 0.1212$, and TSC CSF $p = 1322$. No significant differences in TSC were found between sexes. Although it could be observed that men tend to have lower TSC than woman in all tissues, this difference was not significant (Table 2).

In the second approach, volunteers were divided into 2 age groups: above and below 35 years old. As in the first comparison, there was a significant difference between WM, GM, and CSF in both older and younger groups ($p < 0.001$ in all cases).

Comparing the TSC in the 3 considered tissue types between younger and older volunteers, TSC WM ($p = 0.0085$), TSC GM ($p = 0.0014$), and TSC CSF ($p = 0.0097$). In all these comparisons there was a significant difference in TSC between younger and older volunteers (Figure 6).

Discussion

Different tissue types have different TSC, which means a statistically significant difference between WM, GM, and CSF. This statement holds true in all of the subgroups despite a small number of volunteers in them. It was previously proven [6,23] that most sodium in the brain can be found in CSF and that GM has a higher concentration of sodium than WM; the results in this study are no different in that regard.

There were no differences observed between men and women in TSC in brain tissues. Although the collected data showed that men have slightly lower TSC, that difference is of no significance. According to our knowledge, no previous study analysed the differences between men and women in regards to this parameter, so no data are available for comparison. Dividing participants by age into arbitrarily chosen groups (to maintain roughly equal subgroups) yielded interesting results. As with all previous data, there were differences between TSC in CSF, WM, and GM in all subgroups. Interestingly, there were significant differences ($p < 0.05$) between all these parameters between younger and older participants. Younger volunteers had lower TSC in all calculated parameters. This is in contradiction to findings in another paper [24] in which the mean TSC in the whole brain was stable in all ages in healthy volunteers. Also, some sources [25] point out that overall sodium levels in healthy individuals tend to decrease with age. A possible source of the bias might be in the volunteer group itself. The oldest participant was 64 years of age, and there were

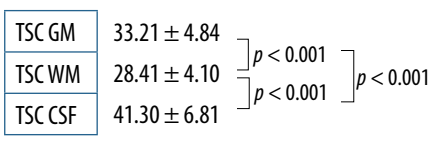

Figure 3. Comparison of TSC values for a whole dataset (mean ± SD)

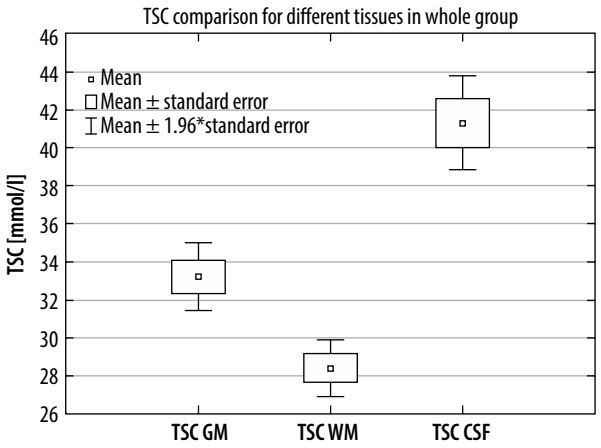

Figure 4. Plot of mean values and standard errors in whole group data

Table 1. Median TSC and quartile in men and women

Median (quartile)	TSC GM	TSC WM	TSC CSF
Women's brains	33.24 (32.12-35.93)	28.15 (26.93-31.58)	40.11 (39.59-46.35)
Men's brains	31.09 (29.95-33.47)	27.16 (25.32-28.47)	39.50 (34.56-42.10)

TSC – tissue sodium concentration, GM – grey matter, WM – white matter, CSF – cerebrospinal fluid

Table 2. Median TSC and quartile in younger and older volunteers

Median (quartile)	TSC GM	TSC WM	TSC CSF
Younger than 35	30.12 (28.59-32.20)	26.33 (25.15-28.12)	38.88 (34.13-39.59)
Older than 35	34.77 (32.54-36.69)	28.93 (27.81-32.01)	41.50 (39.94-45.61)

TSC – tissue sodium concentration, GM – grey matter, WM – white matter, CSF – cerebrospinal fluid.

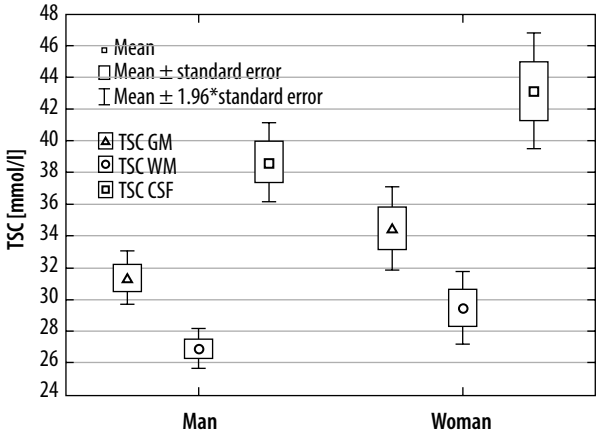

Figure 5. Mean and standard error values of tissues TSC in men and women

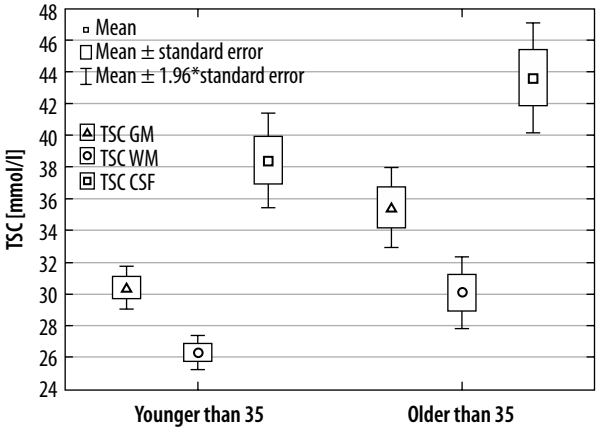

Figure 6. Mean and standard error values of tissues TSC in younger and older groups

only 3 people older than 50 years, which might be a drawback in characterizing the age spread of TSC.

By using a relatively long TR (100 ms), which spanned around 3 times the native sodium relaxation time (25-40 ms), correction for T1 was not of major importance for sodium quantification [26] because negligible T1 saturation occurs in this situation. However, the TE used (2.8 ms) and no correction led to considerable bias, as shown in previous papers [27]. While using a 3D radial GRE sequence a shorter echo time was not achievable. The problem with long TE can be addressed by using one of the more sophisticated sequences developed specifically for ^{23}Na imaging [28]. Because the brain is a homogenous environment and the birdcage coil has a uniform excitation profile, B1 correction was unnecessary. However, even in these conditions, not accounting for B1 inhomogeneity might be considered a drawback. Bearing the above in mind, the values acquired for TSC should be considered as "institutional values" and they can be compared with other values acquired in the same institution, but they might not be comparable with absolute values acquired considering all the mentioned corrections. That being said, values obtained for WM in healthy volunteers in this study are similar to those presented by Romanzetti *et al.* [28] using a similar sequence considering all the above corrections.

Conclusions

The overall acquisition scheme was established, and the entirety of gathered data will be useful in the future as a baseline brain TSC for comparison to values obtained from pathologies.

Conflict of interest

The authors report no conflict of interest.

References

1. Li S, van der Veen JW, An L, et al. Cerebral phosphoester signals measured by 31P magnetic resonance spectroscopy at 3 and 7 Tesla. PLoS One 2021; 16: e0248632.
2. Apps A, Valkovič L, Peterzan M, et al. Quantifying the effect of dobutamine stress on myocardial Pi and pH in healthy volunteers: A 31P MRS study at 7T. Magn Reson Med 2021; 85: 1147-1159.
3. Peterzan MA, Lewis AJM, Neubauer S, et al. Non-invasive investigation of myocardial energetics in cardiac disease using 31P magnetic resonance spectroscopy. Cardiovasc Diagn Ther 2020; 10: 625-635.
4. Lee CY, Soliman H, Geraghty BJ, et al. Lactate topography of the human brain using hyperpolarized 13C-MRI. Neuroimage 2020; 204: 116202.
5. Shammi UA, D'Alessandro MF, Altes T, et al. Comparison of hyperpolarized ^{3}He and ^{129}Xe MR imaging in cystic fibrosis patients. Acad Radiol 2022; 29 Suppl 2: S82-S90.
6. Thulborn KR, Davis D, Snyder J, et al. Sodium MR imaging of acute and subacute stroke for assessment of tissue viability. Neuroimaging Clin N Am 2005; 15: 639-653.
7. Thulborn KR, Lu A, Atkinson IC, et al. Quantitative sodium MR imaging and sodium bioscales for the management of brain tumors. Neuroimaging Clin N Am 2009; 19: 615-624.
8. Bartha R, Megyesi JF, Watling CJ. Low-grade glioma: correlation of short echo time 1H-MR spectroscopy with 23Na MR imaging. Am J Neuroradiol 2008; 29: 464-470.
9. Biller A, Badde S, Nagel A, et al. Improved brain tumor classification by sodium MR imaging: Prediction of IDH mutation status and tumor progression. Am J Neuroradiol 2016; 37: 66-73.
10. Mellon EA, Pilkinton DT, Clark CM, et al. Sodium MR imaging detection of mild Alzheimer disease: preliminary study. Am J Neuroradiol 2009; 30: 978-984.
11. Mohamed SA, Herrmann K, Adlung A, et al. Evaluation of sodium (^{23}Na) MR-imaging as a biomarker and predictor for neurodegenerative changes in patients with alzheimer's disease. In Vivo (Brooklyn) 2021; 35: 429-435.
12. Zöllner FG, Konstandin S, Lommen J, et al. Quantitative sodium MRI of kidney. NMR Biomed 2016; 29: 197-205.
13. Amarteifio E, Nagel AM, Weber MA, et al. Hyperkalemic periodic paralysis and permanent weakness: 3-T MR imaging depicts intracellular 23Na overload-initial results. Radiology 2012; 264: 154-163.
14. Steidle G, Graf H, Schick F. Sodium 3-D MRI of the human torso using a volume coil. Magn Reson Imaging 2004; 22: 171-180.
15. Malzacher M, Kalayciyan R, Konstandin S, et al. Sodium-23 MRI of whole spine at 3 Tesla using a 5-channel receive-only phased-array and a whole-body transmit resonator. Z Med Phys 2016; 26: 95-100.
16. Wetterling F. The detection of infarcted stroke tissue via localised sodium concentration measurements: a non-invasive approach. The University of Dublin 2009.
17. Schneider CA, Rasband WS, Eliceiri KW. NIH Image to ImageJ: 25 years of image analysis. Nat Methods 2012; 9: 671-675.
18. Coupe P, Yger P, Prima S, et al. An optimized blockwise nonlocal means denoising filter for 3-D magnetic resonance images. IEEE Trans Med Imaging 2008; 27: 425-441.
19. Penny WD, Friston KJ, Ashburner JT, et al. (eds.). Statistical Parmetric Mapping-The Analysis of Functional Brian Images by Karl J. Friston. Elsevier, Oxford 2006.
20. Ashburner J, Friston KJ. Unified segmentation. Neuroimage 2005; 26: 839-851.
21. Mazziotta J, Toga A, Evans A, et al. A four-dimensional probabilistic atlas of the human brain. J Am Med Informatics Assoc 2001; 8: 401-430.
22. Jack L. Lancaster PD and MJM. Multi-image Analysis GUI. http://ric.uthscsa.edu/mango/.
23. Madelin G, Lee JS, Regatte RR, et al. Sodium MRI: methods and applications. Prog Nucl Magn Reson Spectrosc 2014; 79: 14-47.
24. Thulborn K, Lui E, Guntin J, et al. Quantitative sodium MR imaging of the human brain at 9.4 Tesla provides assessment of tissue sodium concentration and cell volume fraction during normal ageing. NMR Biomed 2016; 29: 137-143.
25. Miller M. Hyponatremia in the elderly: risk factors, clinical consequences, and management. Clin Geriatr 2009; 17: 34-39.
26. Modo M, Bulte JWM. Magnetic Resonance Neuroimaging. Methods and Protocols. Humana Press 2011.
27. Boada FE, Christensen JD, Huang-hellinger FR, et al. Quantitative in vivo tissue sodium concentration maps: the effects of biexponential relaxation. Magn Reson Med 1994; 32: 219-223.
28. Romanzetti S, Mirkes CC, Fiege DP, et al. Mapping tissue sodium concentration in the human brain: a comparison of MR sequences at 9.4Tesla. Neuroimage 2014; 96: 44-53.